Eur. Phys. J. A **25**, s01, 409–413 (2005)
DOI: 10.1140/epjad/i2005-06-094-0

EPJ A direct
electronic only

Reduced transition probabilities for the first 2^+ excited state in ^{46}Cr, ^{50}Fe, and ^{54}Ni

K. Yamada[1,a], T. Motobayashi[1], N. Aoi[1], H. Baba[2], K. Demichi[3], Z. Elekes[4], J. Gibelin[5], T. Gomi[1], H. Hasegawa[3], N. Imai[1], H. Iwasaki[6], S. Kanno[3], T. Kubo[1], K. Kurita[3], Y.U. Matsuyama[3], S. Michimasa[1], T. Minemura[7], M. Notani[8], T. Onishi K.[6], H.J. Ong[6], S. Ota[9], A. Ozawa[10], A. Saito[2], H. Sakurai[6], S. Shimoura[2], E. Takeshita[3], S. Takeuchi[1], M. Tamaki[2], Y. Togano[3], Y. Yanagisawa[1], K. Yoneda[11], and I. Tanihata[8]

[1] RIKEN, 2-1 Hirosawa, Wako, Saitama 351-0198, Japan
[2] Center for Nuclear Study (CNS), University of Tokyo, RIKEN Campus, 2-1 Hirosawa, Wako, Saitama 351-0198, Japan
[3] Department of Physics, Rikkyo University, 3-34-1 Nishi-Ikebukuro, Toshima, Tokyo 171-8501, Japan
[4] Institute of Nuclear Research of the Hungarian Academy of Sciences, P.O. Box 51, Debrecen H-4001, Hungary
[5] Institut de Physique Nucléare, F-91406 Orsay Cedex, France
[6] Department of Physics, University of Tokyo, 7-3-1 Hongo, Bunkyo, Tokyo 113-0033, Japan
[7] High Energy Accelerator Research Organization, 1-1 Oho, Tsukuba, Ibaraki 305-0801, Japan
[8] Argonne National Laboratory, 9700 S. Cass Avenue, Argonne, IL 60439, USA
[9] Department of Physics, Kyoto University, Kita-Shirakawa-Oiwake, Sakyo, Kyoto 606-8502, Japan
[10] Department of Physics, University of Tsukuba, 1-1-1 Tennoudai, Tsukuba, Ibaraki 305-8577, Japan
[11] National Superconducting Cyclotron Laboratory, Michigan State University, East Lansing, MI 48824-1321, USA

Received: 22 December 2004 /
Published online: 27 May 2005 –

Abstract. We measured $B(E2; 0^+_{\rm g.s.} \rightarrow 2^+_1)$ values for the proton-rich ^{46}Cr, ^{50}Fe, and ^{54}Ni nuclides by intermediate-energy Coulomb excitation in order to study the systematic behavior of collectivity in the $Z = 20$–28 region. The present study completes the $B(E2)$ values for the $T_z = \pm 1$ even-even pair nuclei up to $Z = 28$. The double ratios of proton and neutron matrix elements, $(|M_{\rm n}|/|M_{\rm p}|)/(N/Z)$, have been extracted from the $B(E2)$ values combining with the ones of their mirror nuclei, and compared with theoretical predictions.

PACS. 25.70.De Coulomb excitation – 23.20.Lv γ transitions and level energies

1 Introduction

Systematic behaviors of the reduced transition probability $B(E2)$ and energy $E(2^+)$ for the first excited state in even-even nuclei provide useful information for investigating the evolution of the nuclear collectivity. These properties were extensively studied for the isotopes on and near the stability line, and expanded mainly into the neutron-rich region. However, the experimental studies for excited states have not so often been performed in the proton-rich region because of the relatively poor quality for available RI beams. Thus, the systematics of $B(E2)$ for isospin $T_z = \pm 1$ even-even pairs had only been completed up to $A = 42$ mass system. The aim of the present study is to extend the systematics of $B(E2)$ and $E(2^+)$ up to ^{56}Ni along the $N = Z$ line in order to clarify the collective aspects in the beginning of *pf* shell up to $N = Z = 28$ double shell closure.

To complete the systematics in that region, one should measure the $B(E2)$ values for ^{46}Cr, ^{50}Fe, and ^{54}Ni, and the $E(2^+)$ value for ^{54}Ni. The $E(2^+)$ values for the ^{46}Cr and ^{50}Fe were deduced to be 892 keV [1] and 765 keV [2], respectively, by using HPGe detectors. Recently, the $B(E2\uparrow)$ and $E(2^+)$ values for the ^{54}Ni have been reported by Yurkewicz *et al.* [3] to be 626(169) e^2fm^4 and 1396(9) keV. Their mirror nuclei, ^{46}Ti, ^{50}Cr, and ^{54}Fe, are all stable, and their $B(E2)$ and $E(2^+)$ values are well known.

In the present work, we performed in-beam γ-ray spectroscopy of ^{46}Cr, ^{50}Fe, and ^{54}Ni with intermediate-energy Coulomb excitation using inverse kinematics. The fraction of these proton-rich nuclei in secondary beams produced by the projectile fragmentation is too low for direct experimental measurement. To increase the fraction, we constructed a Radio Frequency (RF) deflector system [4] for purification of the secondary beams. The $B(E2)$ values were extracted from the Coulomb excitation cross-sections by Distorted-Wave Born Approximation (DWBA) analysis. In order to study general trends of collectivity, the

[a] Conference presenter; e-mail: nari-yamada@riken.jp

proton and neutron matrix elements, $M_{\rm p}$ and $M_{\rm n}$, were separately extracted from the $B(E2)$ values by using Bernstein's mirror nucleus method [5], which is based on the equality between the $M_{\rm p}$ and $M_{\rm n}$ in the mirror pair under the assumption of isospin symmetry.

2 Experimental procedure

The experiment was carried out at the RIKEN Accelerator Research Facility. Secondary beams of ^{46}Cr, ^{50}Fe, and ^{54}Ni were produced by the projectile fragmentation of a ^{58}Ni primary beam accelerated up to 95 MeV/nucleon by the RIKEN Ring Cyclotron. The primary beam irradiated a nickel target of 303 mg/cm^2 thickness with a typical beam intensity of 4.0 pnA. Each fragment was separated by the RIKEN Projectile-Fragment Separator (RIPS) [6] with a wedge-shape aluminum degrader of 116 mg/cm^2 thickness. The fraction of ^{46}Cr, ^{50}Fe, and ^{54}Ni in the secondary beam were only 0.1%, 0.05%, and 0.02%, respectively. These secondary beams were purified by the RF deflector system located around the second focal plane (F2) of RIPS.

The RF deflector system consists of an electrode part and a variable separation slit (Y-SLIT). After the selection by the magnetic rigidity, each nuclide in the secondary beam has a different velocity. Thus, we can use the difference of flight time between the production target and F2. A vertically arranged parallel-electrode is set along the beam line, and high alternating voltage with sinusoidal form is applied to the electrode in the direction perpendicular to the beam axis. Since the arrival time of particles at F2 depends on the species, a particle passing through the electrode is deflected by an amount depending on the species. When the oscillation phase is adjusted so as to permit the nucleus of interest to pass through the electrodes without deflection, other contaminants coming in the electrodes are deflected by the electric field and stopped on the Y-SLIT placed downstream of the electrodes. The RF deflector was operated at a voltage of 100 kV with a frequency of 14.05 MHz, synchronized with the RF signal of the injector cyclotron. The momentum spread of each secondary beam was set to $\pm$0.7%, and the Y-SLIT was set to limit the total beam intensity to 1×10^4 counts per second. Fractions of ^{46}Cr, ^{50}Fe, and ^{54}Ni beams were about ten times improved to 1.0%, 0.5%, and 0.2% by the RF deflector, respectively. These secondary beams had typical intensities of 40 counts per second, 60 counts per second, and 10 counts per second on the reaction target, respectively.

A lead target was used to study Coulomb excitation. The thickness was 224 mg/cm^2 for the measurement of ^{46}Cr and ^{50}Fe, and the one for ^{54}Ni was 189 mg/cm^2 thick. The beam energies were 44 MeV/nucleon, 41 MeV/nucleon, and 42 MeV/nucleon in the middle of the lead target, respectively.

Particle identification of the incident beam was performed on an event-by-event basis by measuring the time-of-flight (TOF) information using a 0.1 mm plastic scintillator placed at the final focal plane (F3) of RIPS and cyclotron RF signals. The plastic scintillator had an active area of 80$\times$80 mm^2, and the scintillation light was detected by two photomultiplier tubes from both ends of the scintillator. The fluxes of the incident beams were also counted by this scintillator. We placed a 325-μm-thick silicon detector with an active area of 50$\times$50 mm^2 at F3 to make separate runs for measuring the fraction of the nucleus of interest in the beam. The incident angle of the beam was measured by a set of two delay-line Parallel-Plate Avalanche Counters (PPACs) [7] with a sensitive area of 100$\times$100 mm^2 installed at F3. The two PPACs were placed 30 cm apart along the beam line. The typical position resolution of the PPACs was about 1.0 mm in FWHM. Another PPAC of the same type was placed behind the Y-SLIT in order to monitor the beam deflection in the vertical direction.

Outgoing particles were detected by a delay-line PPAC with 150$\times$150 mm active area (PI-PPAC) and nine sets of PIN silicon-detector telescope in order to select inelastic-scattering events. The PI-PPAC was located 57 cm downstream of the reaction target, and its position information was used to determine the scattering angle, combined with the one from the two PPACs in beam line. The silicon-detector telescope was placed 62 cm downstream of the reaction target, which was arranged as a 3$\times$3 matrix with three layers consisting respectively of 325 μm thick-, 500 μm thick-, and 500 μm thick-detectors. All silicon detectors had the same active area of 50$\times$50 mm^2 with single electrode and were mounted on 56$\times$56 mm^2 frames. The telescope covered the angles up to 7.2 degrees with respect to the beam axis, which sufficiently accepted most of inelastically scattered particles. The particles were identified from energy deposits in the first and second layers of the silicon detectors by the ΔE-E method. The third layer was used as veto to reject light particles passing through the second layer. To estimate the acceptance of the silicon telescope, we performed a Monte Carlo simulation, which took into account the detector geometry including frames between the silicon detectors, the finite size and angular spread of the incident beam, the multiple scattering in the reaction target, and the theoretical angular distribution of Coulomb excitation calculated by the coupled-channel code ECIS97 [8]. In order to check the accuracy of the simulation, we compared the simulated acceptance with the one deduced from interpolating the spatial distribution of scattered particles at the silicon telescope obtained from the image at the PI-PPAC. They agreed with 3% accuracy.

De-excitation γ-rays were measured by using a subset of DALI2[1] [9] consisting of 116 NaI(Tl) scintillators with eleven layers. The array surrounded the target from 44 to 156 degrees with respect to the beam axis. Each scintillator crystal had a size of 8$\times$4.5$\times$16 cm^3 coupled to a 3.8 cm $\varnothing$ photomultiplier tube. Lead blocks with 50 mm thickness were placed just downstream of the NaI(Tl) array to reduce the background γ-rays from the silicon telescope. The high granularity of the setup allowed us to measure the angle of γ-ray emission with approximately 10-degree accuracy. The angle information was used to

[1] Detector Array for Low Intensity radiation 2.

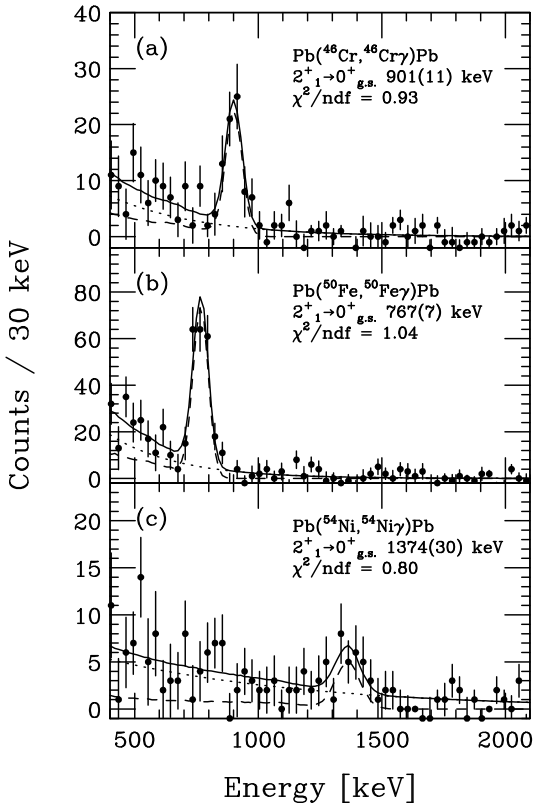

Fig. 1. Doppler-corrected γ-ray spectra obtained for the Coulomb excitation of ^{46}Cr (a), ^{50}Fe (b), and ^{54}Ni (c). The solid curves are fits to the data, which contain the simulated line shapes for γ-rays (dashed curves) and exponential background contributions (dotted curves).

Table 1. $E(2^+)$ and $B(E2\uparrow)$ values deduced from the present experiment together with their previous ones.

	$E(2^+)$ (keV)		$B(E2\uparrow)$ (e^2fm^4)	
Nucleus	Present	Previous	Present	Previous
^{46}Cr	900(10)	892	930(200)	–
^{50}Fe	767(7)	765	1400(300)	–
^{54}Ni	1370(30)	1396(9)	590(170)	626(169)

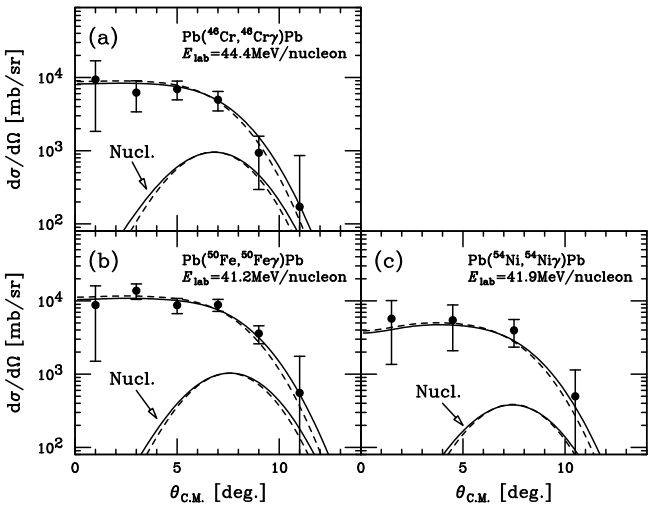

Fig. 2. Differential cross-sections for Pb induced inelastic excitation of ^{46}Cr (a), ^{50}Fe (b), and ^{54}Ni (c). The solid (dashed) curves represent calculated ones using the optical-potential set A (B).

correct for the large Doppler shift of γ-rays emitted from the particles in flight with $\beta = v/c \approx 0.3$. The intrinsic energy resolution of each detector and the total photopeak efficiency of DALI2 were typically 9.2% FWHM and 18.1% for 662 keV photons from a ^{137}Cs standard source. The absolute efficiencies were also obtained by a Monte Carlo simulation using the GEANT3 code [10], which were compared with the ones for source data in order to confirm the accuracy of the simulation. The results were consistent with the source data within 5% errors. The detection efficiency of DALI2 for the γ-rays emitted from moving nuclei are simulated and used to extract the Coulomb excitation cross-sections.

3 Result and discussion

Figure 1 shows the Doppler-corrected γ-ray spectra measured in coincidence with the scattered particles of ^{46}Cr, ^{50}Fe, and ^{54}Ni. A single distinct peak is observed in each spectrum, and their energies have been determined to be 900(10) keV, 767(7) keV, and 1370(30) keV, respectively. The present results agree with their previously reported values, 892 keV, 765 keV, and 1396(9) keV, respectively.

The angle-integrated cross-sections were determined from the γ-ray yields after correcting for the detection efficiencies. The yields were evaluated by an analysis with a function $y = af(E_\gamma) + b \cdot \exp(-cE_\gamma)$, where $f(E_\gamma)$ is the spectral shape obtained by the GEANT simulation, and a, b, and c are free parameters. Results of the fits are shown by the solid curves in fig. 1 together with their individual components. The data are well reproduced by the sum of the two components. The cross-sections for ^{46}Cr, ^{50}Fe, and ^{54}Ni were deduced to be 460(90) mb, 690(120) mb, and 300(80) mb, respectively.

The DWBA analysis was performed using the ECIS97 code assuming the collective deformation model. For the calculation, we used two different optical-potential parameter sets A and B, respectively obtained from the elastic scattering of ^{40}Ar on ^{208}Pb at 44 MeV/u [11] and ^{58}Ni on ^{208}Pb at 17 MeV/u [12]. The $B(E2)$ values were extracted by taking the average of the calculations obtained with the two potential sets, and their differences were included in the error. The resultant $B(E2; 0^+_{\rm g.s.} \rightarrow 2^+_1)$ values are 930 ± 200 e^2fm^4, 1400 ± 300 e^2fm^4, and 590 ± 170 e^2fm^4 for ^{46}Cr, ^{50}Fe, and ^{54}Ni, respectively. The complete systematics of $B(E2)$ for the $T_z = \pm 1$ even-even pairs up to $Z = 28$ has been established by the present study. The results of $E(2^+)$ and $B(E2\uparrow)$ are listed in table 1 together with their previous values.

The validity of the DWBA calculation was examined by comparing with the angular distribution of differential

cross-sections. The results are shown in fig. 2. The experimental data exhibit typical angular dependence for the $E2$ Coulomb excitation. Theoretical angular distributions calculated by the ECIS97 code assuming Coulomb excitation are shown for the potential A (B) by the solid (dashed) curves. The components of nuclear excitation are also shown by solid or dashed curves in each figure. These calculated cross-sections are smeared by angular resolution of the measurement, 1.2 degrees. As shown in the figure, the calculation reproduces well the experimental data, and hence, indicates the applicability of the DWBA calculation. In addition, the results indicates a negligibly small contribution from the nuclear excitation and $E2$ dominance in the present cases.

The angular distribution of γ-ray emission was analyzed to check a possible influence to the cross-section evaluation. The experimental distribution was compared with the one obtained from a statistical tensor calculated by the ECIS97 assuming the $2^+ \rightarrow 0^+$ transition. From the comparison, the anisotropy of the angular distribution was found to affect only 5% of the evaluation assuming an isotropic emission, indicating a good coverage of detection angle in the present experiment.

The double ratio $(|M_\mathrm{n}|/|M_\mathrm{p}|)/(N/Z)$ is a measure for the collectivity of the 2_1^+ states. In even-even nuclei in which both proton and neutron shells are open, the ratio is generally close to unity, while nuclei with closed shells systematically deviate from unity. To evaluate the ratios, the $|M_\mathrm{p}|$ values for ^{46}Cr, ^{50}Fe, and ^{54}Ni were extracted from the $B(E2)$ values by taking their square root as 4.4 ± 0.5, 5.1 ± 0.5, and 3.1 ± 0.4, respectively, in single-particle units $B_\mathrm{sp}(E2\uparrow) = 0.297A^{4/3}\ e^2\mathrm{fm}^4$. The $|M_\mathrm{n}|$ values were obtained from the square root of $B(E2)$ values for their mirror nuclei [13] to be 4.4 ± 0.1, 4.4 ± 0.1, and 3.2 ± 0.1 in the single-particle units for ^{46}Cr, ^{50}Fe, and ^{54}Ni, respectively. Figure 3 shows the results of $(|M_\mathrm{n}|/|M_\mathrm{p}|)/(N/Z)$ for $T_z = -1$ even-even nuclides in the $Z = 10$–28 region. In the figure, the ratios fairly deviate from unity near the closed shells and follow the trend expected for nuclei close to the shell closure. The results obtained for both ^{46}Cr and ^{50}Fe are close to unity and are consistent with the pictures of collective nuclei without neutron and proton shell closures. The ratio for ^{54}Ni, which is close to unity, indicates the weakness of the $Z = 28$ shell closure.

In fig. 3, the ratios are compared with theoretical predictions. The dashed lines indicate the results by the shell-model calculations. The results using the USD interaction by Brown and Wildenthal [14] are shown in the *sd*-shell region, while the results calculated by Honma *et al.* [15] using GXPF1 interaction with $e_\mathrm{p} = 1.5$ and $e_\mathrm{n} = 0.5$ are plotted in the *pf*-shell region. The dot-dashed line indicates the ratios extracted from the intrinsic electric quadrupole moment predicted by Sagawa *et al.* [16] using the deformed Hartree-Fock + BCS calculation with SIII interaction. The tendency of the systematic behavior for $(|M_\mathrm{n}|/|M_\mathrm{p}|)/(N/Z)$ values is reproduced by these predictions. However, the experimental results exhibit smaller extents of single-particle natures compared with the shell-model predictions in the vicinity of the shell closure 20 and 28, suggesting the importance of collective aspects which should be taken into account. Better agreements are obtained by the deformed HF + BCS prediction. However, it considerably underestimates the amplitude of the matrix elements: for example, the predicted $|M_\mathrm{p}|$ values are smaller by a factor of about 20 for ^{38}Ca and ^{42}Ti.

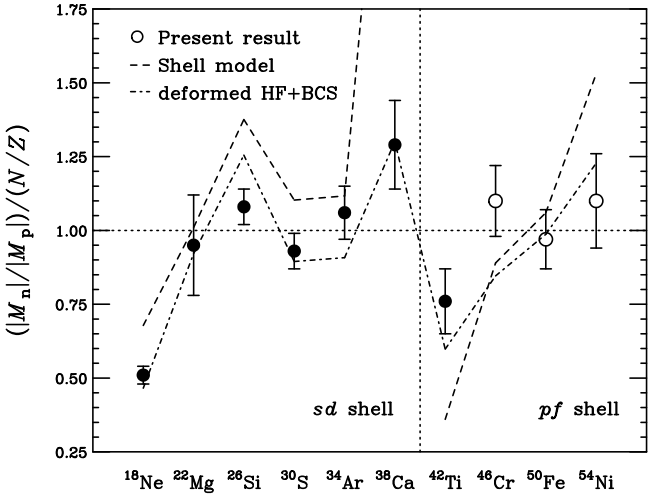

Fig. 3. The double ratio $(|M_\mathrm{n}|/|M_\mathrm{p}|)/(N/Z)$ for $T_z = -1$ even-even nuclides in the $Z = 10$–28 region. The open circles indicate the ratios extracted from the present results. The closed circles are obtained from the $B(E2)$ values in ref. [13].

4 Summary

We have measured the $B(E2)$ values for ^{46}Cr, ^{50}Fe, and ^{54}Ni by intermediate-energy Coulomb excitation. The RF deflector system enables efficient measurements for these proton-rich nuclei. The present study completes the systematics of experimental $B(E2)$ values for the isospin $T_z = \pm 1$ even-even pair nuclei up to $Z = 28$. Using the data of their mirror nuclei, the double ratios of matrix elements $(|M_\mathrm{n}|/|M_\mathrm{p}|)/(N/Z)$ have been extracted up to $A = 54$ system. The present result suggests the necessity of more elaborate treatment of the nuclear collectivity in this mass region.

The authors are grateful to the researchers and staffs in the RIKEN Accelerator Research Facility for their valuable advice and collaboration.

References

1. P.E. Garrett *et al.*, Phys. Rev. Lett. **87**, 132502 (2001).
2. S.M. Lenzi *et al.*, Phys. Rev. Lett. **87**, 122501 (2001).
3. K.L. Yurkewicz *et al.*, Phys. Rev. C **70**, 054319 (2004).
4. K. Yamada *et al.*, Nucl. Phys. A **746**, 156c (2004).
5. A.M. Bernstein *et al.*, Phys. Rev. Lett. **42**, 425 (1979).
6. T. Kubo *et al.*, Nucl. Instrum. Methods Phys. Res. B **70**, 309 (1992).

7. H. Kumagai *et al.*, Nucl. Instrum. Methods Phys. Res. A **470**, 562 (2001).
8. J. Raynal, Coupled channel code ECIS97, unpublished.
9. S. Takeuchi *et al.*, RIKEN Accel. Prog. Rep. **36**, 148 (2003).
10. *GEANT3: Detector Description and Simulation Tool* (CERN, Geneva, 1993).
11. N. Alamanos *et al.*, Phys. Lett. B **137**, 37 (1984).
12. M. Beckerman *et al.*, Phys. Rev. C **36**, 657 (1987).
13. S. Raman *et al.*, At. Data Nucl. Data Tables **78**, 1 (2001).
14. B.A. Brown *et al.*, Phys. Rev. C **26**, 2247 (1982).
15. M. Honma *et al.*, Phys. Rev. C **69**, 034335 (2004).
16. H. Sagawa *et al.*, submitted to Phys. Rev. C.